VVV Survey – ESO Phase 3
VVV Infrared Astrometric Catalogue (VIRAC) v2 release

Abstract

We describe the VIRAC2 catalogue of proper motions, parallaxes, and light curves (Smith et al. 2025) based on VVV and VVVX survey data, in the form that is provided in the ESO archive. The VVV survey (ESO programme 179.B-2002) spanned a 5-year period (2010-2015) and observed approx. 560 deg2 of the southern Galactic plane and bulge. The VVVX survey (ESO programme 198.B-2004), extended this to cover a combined 1700 deg^2, and the additional epochs in the original area roughly doubled the total epoch baseline. VIRAC2 is a catalogue of positions, proper motions, parallaxes and ZYJHK$_s$ near-infrared photometric and astrometric time series for 545,346,537 unique stars. The catalogue is based on a point spread function fitting reduction of observations covering the original VVV footprint only but incorporating additional VVVX epochs from 2016-2019. It uses Gaia DR3 as an external astrometric reference catalogue, and hence astrometry is on an absolute reference frame, in contrast to VIRAC v1. We adopted a global photometric calibration algorithm, using 2MASS as an external photometric reference catalogue, with an additional non-astrophysical noise reduction stage. It is complete at the >90 per cent level for 11 < K$_s$ mag < 16 sources but extends to K$_s$ ≈ 17.5 mag in most fields. This is approximately 1 magnitude deeper than VIRAC v1. The 1σ astrometric performance for 11 < K$_s$ mag < 14 sources is typically ≈ 0.37 mas yr^{-1} per dimension for proper motion, and 1 mas for parallax. At K$_s$ = 16 the equivalent values are around 1.5 mas yr^{-1} and 5 mas. These uncertainties are validated against Gaia DR3 and Hubble Space Telescope astrometry, and are roughly halved relative to VIRAC v1 due to the longer epoch baseline and pipeline enhancements. Complete descriptions of the VIRAC2 data and pipeline methods are available in Smith et al. (2025).

Overview of Observations

The VISTA Variables in the Via Lactea Survey and its extension (VVV, Minniti et al. 2010; VVVX Saito et al. 2024) were conducted with the 4m VISTA telescope at Cerro Paranal using the VISTA Infrared Camera (VIRCAM; Dalton et al. 2006; Sutherland et al. 2015). VIRCAM consists of sixteen 2048 x 2048 pixel arrays, and in conjunction with VISTA images a total area of 0.6 square degrees at each pointing position or 'pawprint'. Detectors are arranged in a 4 x 4 grid with spacings of 90% of a detector width in the *Y* dimension and 42.5% of a detector width in the *X* dimension. The conventional VIRCAM tiling pattern consists of six of these pawprints (three offset in *X* and two in *Y*) that fill a VIRCAM 'tile' when stacked. VIRCAM tiles are approximately 1.4 x 1.1 degrees. Most positions in a VIRCAM tile are observed twice due to the ≈50% pawprint overlap in the *X* direction.
The Cambridge Astronomical Survey Unit (CASU) provides pipeline data reduction and calibration of their aperture photometry and astrometry for individual pawprint images via the VISTA Data Flow Pipeline (Irwin et al. 2004), see also Lewis et al. (2010) and http://casu.ast.cam.ac.uk/surveys-projects/vista/technical.

VIRAC2 used 179,403 VVV and 18,020 VVVX pawprint stack observations spanning 30th January 2010 to 1st September 2019 in the Z, Y, J, H and K$_s$ passbands. These are the only observations that passed our basic quality control selection criteria. The images are available in the ESO archive and separately in the VISTA Science Archive at vsa.roe.ac.uk. Only observations covering the original VVV area were used, these encompass the regions defined approximately by 295 < l° < 350, |b°| < 2 (i.e. the Galactic disc fields), and 10 < l° < 350, -10 < b° < 5 (i.e. the Galactic bulge fields). Figure 1 is a map showing the

VVV area including the tile numbers for reference, but tile numbers are not used by the VIRAC2 pipeline. The map shown in Figure 1 overlaps the extinction map from Schlegel et al., 1997.

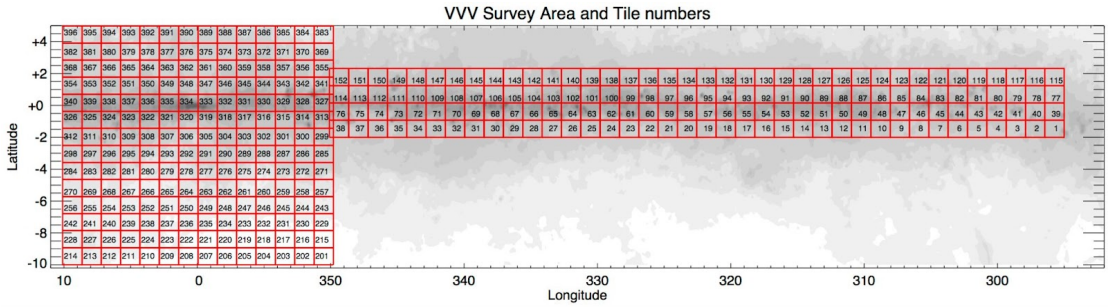

Release Content

The VIRAC2 catalogues cover approx. 560 contiguous square degrees of the southern Galactic disc and bulge in the Z, Y, J, H, and K_s bandpasses, using data obtained between 30th January 2010 to 1st September 2019. The limiting magnitude varies, typically due to varying source density, but is approximately 17.5 mag in the K_s bandpass in most fields. Sanders et al. (2022) determine that the catalogue is at least 90% complete to $K_s = 16$ mag everywhere except for a few square degrees in the vicinity of the Galactic centre. The K_s images were used for source detection, with the other bandpasses being incorporated through crossmatching, taking source motion into account.

The VIRAC2 catalogues are split into five database tables in the ESO archive. These are:

I. `VVVX_VIRAC_V2_SOURCES`,

II. `VVVX_VIRAC_V2_REJECTED_SOURCES`,

III. `VVVX_VIRAC_V2_LC`,

IV. `VVVX_VIRAC_V2_REJECTED_LC`, and

V. `VVVX_VIRAC_V2_OBS`.

Where tables (i) and (ii) are the aggregate source data (e.g. positions, proper motions, mean photometry), tables (iii) and (iv) are the time series data (photometric and astrometric), and table (v) contains observation-related information (e.g. image filename, seeing). The content of the source and time series catalogues is further split into main and rejected selections. The raw catalogue contained junk rows for a variety of reasons (e.g. duplicates, erroneous detections in the wings of the PSFs of bright stars, etc.), and these were separated into the rejected tables to the best of our ability. The rejected tables are included since some interesting sources (e.g. photometric transients) were known to have failed our quality control criteria for legitimate reasons. See Smith et al. (2025) for more details. Tables (i) and (iii) are the main selection, and tables (ii) and (iv) are the rejected selection.

The volume of the five tables is shown in the table below.

table name	row count	data volume (FITS)
`VVVX_VIRAC_V2_SOURCES`	545,346,537	195G
`VVVX_VIRAC_V2_REJECTED_SOURCES`	844,909,541	300G

VVVX_VIRAC_V2_LC	95,768,366,366	11T
VVVX_VIRAC_V2_REJECTED_LC	27,419,652,812	3T
VVVX_VIRAC_V2_OBS	197,423	28M

In addition to the VIRAC2 data, this release also includes 24,194 pawprint images and their associated source tables and confidence maps. These were used to generate the VIRAC2 data product but were missing from previous releases, mainly due to differences in criteria used to select sufficiently high quality observations.

Release Notes

Data Reduction and Calibration

Pipeline processing started with pawprint images and automated source detection, flux and positional measurement using the DoPhot point spread function (PSF) fitting software (Schechter et al. 1993, Alonso-García et al. 2012). This process yielded 114 billion tentative source detections from the 197,423 images.

Astrometric calibration was performed on a per-detector, per-observation basis. Sources were cross-matched to Gaia DR3 using their CASU astrometric solutions. The astrometry was then refined through fitting and application of Chebyshev polynomials of one of a number of degrees, selected to minimise overfitting given the widely varying availability of reference stars. DoPhot centroid uncertainties were propagated through the polynomials to produce uncertainties in equatorial positions, which were then rescaled such that their distribution matched that of the residuals to the polynomial fitting.

Inter-observation source matching, i.e. time-series production, and mean astrometry fitting was performed next. This processing was performed within 22,585 healpixels of various sizes covering the target area, each incorporating a small external border to take into account sources straddling the boundaries. An initial inter-observation matching was conducted, taking into account source motions within a seed star catalogue (e.g. VIRAC v1, Gaia, previous pipeline runs) where they existed, and mean field motions where they did not. This produced a list of sources which should be largely complete but was expected to be highly contaminated by incorrect inter-observation matches and duplicated sources. What followed was an iterative process of fitting of mean astrometric parameters (reference position, proper motion and parallax), and re-matching of the source list to the catalogues to refine the source list. The process meant that the time-series of individual sources tended to converge to a clean set. Most duplicate sources became obvious as their time series were identical, in which case the duplicates were removed. Where a time-series did not change between iterations it was judged to have converged and the sequence of observations and its mean astrometry was recorded.
Some less obvious duplicates remained, those with similar albeit non-identical time series and positions. These are flagged in the catalogues. Individual detections which are shared between multiple sources (e.g. in the case of blending) are also flagged as such. An approximate number of observations of each source in each bandpass is provided, having been produced using their predicted positions and an average CASU confidence map.

The main photometric calibration is performed using a global minimisation algorithm, which is made possible due to the 50% overlap between pawprints inherent in the VIRCAM tiling pattern. The five bandpasses are calibrated independently of each other. Isolated 2MASS reference stars from regions of low interstellar extinction are selected, and their magnitudes in the VISTA photometric system are computed using the equations of González-Fernández et al. (2018). These and their counterparts in the VIRAC2 catalogue are used as zero point reference stars. Our

photometric model also includes an illumination map per-detector, and a per-observation, per-detector photometric offset. The former accounts for non-uniform illumination of the focal plane array, and the latter accounts for changing atmospheric conditions, instrument throughput, etc. Model coefficients are optimised over the entire survey by minimising the magnitude difference between successive observations of a set of high quality VIRAC2 reference stars. This process benefits from the overlaps between adjacent pawprint images within and between the survey tiles, thereby minimising non-uniformities in photometric calibration.

A secondary photometric calibration was also performed to reduce high spatial and temporal frequency coherent structure that was evident in maps of residuals to the primary photometric calibration. This was performed in much the same manner as the astrometric calibration above, albeit using the average magnitudes of reliable VIRAC2 stars as a reference catalogue, and served to reduce non-astrophysical scatter in their photometric time series. Their photometric uncertainties were also scaled such that their distribution matched the distribution of residuals to this secondary calibration.

Further detail regarding the data reduction and calibration can be found in Smith et al. (2025).

Data Quality

Peak astrometric performance is in the $11 < K_s$ mag < 14 range, where proper motion uncertainties are typically better than 0.5 mas yr^{-1} per dimension (median 0.36 and 0.38 mas yr^{-1} for ra-cosdec and dec, respectively) and parallax uncertainties are typically around 1 mas (median 1.02 mas). Saturation impacts performance for stars brighter than this. Performance at $K_s = 16$ is typically around 1.5 mas yr^{-1} per dimension for proper motion and 5 mas for parallax.

Mean astrometry and uncertainties were validated against Gaia DR3 (see Smith et al. 2025 for details), and also independently against Gaia DR3 and Hubble Space Telescope proper motions by Luna et al. (2023).

Known issues

In the special case of large amplitude variable sources in crowded fields, the astrometric solution could be unreliable due to systematic changes in the location of the centroid found by DoPhot. This could occur if stars adjacent to the variable star were no longer detected when the latter became much brighter. This issue was noted by Lucas et al. (2024), in the context of highly variable giant stars in the Nuclear Disc of the Milky Way. In general, strongly blended sources with separate catalogue entries can have accurate astrometry but this is not guaranteed. Visual inspection of the time series of RA and Dec coordinates, and the light curve, can be helpful to check the reliability of proper motions and parallaxes, given that an approximately linear motion across the sky is expected for the vast majority of stars and position should not correlate with source magnitude.

Population studies can be performed with relative confidence, but we caution that attempts to select outliers (e.g. high proper motion or parallax sources and large amplitude variable sources) will tend to also preferentially select the erroneous examples. Care must be exercised in cleaning such samples.

Previous Releases

The previous release, VIRAC version 1, is also available from the ESO archive. The relevant release description can be acquired here:
http://www.eso.org/rm/api/v1/public/releaseDescriptions/138

VIRAC version 2 differs significantly from version 1, in all areas of the pipeline and data model. The principal changes are: (in the following points v1 refers to VIRAC version 1 and v2 refers to VIRAC version 2)

- Where v1 processing began with object catalogues produced by CASU using their aperture-based imcore software, v2 began with images and used the PSF fitting based DoPhot software. This yielded 1 mag (approx) of additional depth and an improved handling of blended stars, but did result in a slightly higher incidence of missing saturated stars.

- v2 uses an entirely new inter-observation matching and unique-source identification algorithm. The main impacts of this are that a) inter-observation matching has (in principle) no upper limit on proper motion, and b) source identifiers are not common between v1 and v2. Due to (b), cross matching between versions must be done using equatorial coordinates.

- No suitable external astrometric reference catalogue was available for v1, hence **v1 proper motion measurements were relative to the average motions of local reference stars**. Average motions were always offset from zero (zero being defined by an external frame composed of 'static' sources e.g. quasars) by up to a few milliarcseconds per year due to Galactic rotation and Solar peculiar motion. By contrast, v2 is anchored to Gaia DR3 and takes Gaia proper motion and parallaxes into account. Since Gaia astrometry is relative to a static external reference frame, with low systematic offsets relative to this, hence **v2 can be considered to be relative to a static external reference frame**.

- An entirely new astrometric calibration algorithm was developed for v2.

- While v1 provided parallax measurements for only sources that exhibited significant proper motion, v2 includes and fits for parallax in the astrometric model of all stars detected at ten or more epochs, i.e. ten or more pawprint stack images in the Ks bandpass. This corresponds to all stars in the `VVVX_VIRAC_V2_SOURCES` table.

- The reference epoch for mean astrometry fitting is 2014.0 for v2, whereas it was 2012.0 for v1.

- v2 incorporated additional observations of the original VVV area from the VVVX survey, thereby roughly doubling the epoch baseline. As a consequence of this and other upgrades to the pipeline astrometric precision is roughly doubled relative to v1.

- Where v1 adopted the CASU photometric calibration, v2 uses a new global photometric calibration algorithm that is anchored back to 2MASS (and adopting the transformations in González-Fernández et al., 2018). Additionally, v2 benefits from a secondary noise reduction algorithm intended to reduce non-astrophysical variability in photometric light curves.

- The data model of v2 bears little resemblance to that of v1.

Data Format

File Types

All images and catalogues are distributed in FITS format.
Four of the catalogues are in multi-tile fashion format, all of them consisting of 22,583 FITS catalog tiles, while the observation one is monolithic, as defined in the Phase3 SDPS (http://www.eso.org/sci/observing/phase3/p3sdpstd.pdf).
Individual tiles correspond to an area defined by a given healpixel at a given resolution, specified by the pixel ID and the nsides parameter. The resolution varies by sky location to try to keep file sizes somewhat similar given local source density and epoch count, but is always one of nsides=[256,512,1024].

Files can be retrieved separately via the ESO graphical interface ASP (https://archive.eso.org/scienceportal), or programmatically. The whole catalog content can be accessed and queried as a unique table via the Catalog Facility (https://www.eso.org/qi) or programmatically.

The naming convention used for the released files is the following:

- Observation catalogue:
  1 file
  VIRAC2_catalogue_index.fits

- Source catalogue:
  22583 files
  VIRAC2_n[xxx]_[yyyyyy]_sources.fits

- Rejected source catalogue:
  22583 files
  VIRAC2_n[xxx]_[yyyyyy]_rejected_sources.fits

- Light curves catalog
  22583 files
  VIRAC2_n[xxx]_[yyyyyy]_time_series.fits

- Light curves of the rejected sources
  22583 files
  VIRAC2_n[xxx]_[yyyyyy]_rejected_time_series.fits

Where [xxx] is the nsides parameter of the healpixel, and [yyyyyy] is the pixel ID. e.g.:
VIRAC2_n256_668768_time_series.fits

The additional 72582 imaging products (4.4T) released are in the standard VISTA format.

SCIENCE.MEFIMAGE	fits.fz	24194	1.58T
SCIENCE.SRCTBL	fits	24194	2.19T
ANCILLARY.WEIGHTMAP	fits.fz	24194	0.62T

Catalogue Columns

VVVX_VIRAC_V2_SOURCES and VVVX_VIRAC_V2_REJECTED_SOURCES table schema:
Column names, units and descriptions for the source tables. An example row is also given. The *sourceid* field links to the light curve table (see below). This format is the same for both the main and reject tables.

Column Label	Units	Description	Example Row
sourceid		unique source identifier	15869033004249
astfit_epochs		number of epochs used for astrometric solution	180
astfit_params		number of astrometric solution parameters	5
duplicate		flag indicating a likely duplicate entry	0
ref_epoch	yr	astrometric reference epoch	2014
ra	deg	right ascension	229.3392813
ra_error	mas	uncertainty on right ascension	0.4829365389
de	deg	declination	-58.85879996
de_error	mas	uncertainty on declination	0.7933554229

parallax	mas	trigonometric parallax	31.56454217
parallax_error	mas	uncertainty on trigonometric parallax	0.966160276
pmra	mas/yr	proper motion in right ascension times cos(dec)	-94.70174133
pmra_error	mas/yr	uncertainty on proper motion in right ascension times cos(dec)	0.3482852735
pmde	mas/yr	proper motion in declination	-134.8485741
pmde_error	mas/yr	uncertainty on proper motion in declination	0.3454985426
ra_de_corr		correlation between ra and de	0.029712955
ra_parallax_corr		correlation between ra and parallax	0.33010614
ra_pmra_corr		correlation between ra and pmra	0.2891742
ra_pmde_corr		correlation between ra and pmde	0.011853172
de_parallax_corr		correlation between de and parallax	0.09001031
de_pmra_corr		correlation between de and pmra	0.0033594724
de_pmde_corr		correlation between de and pmde	-0.032637153
parallax_pmra_corr		correlation between parallax and pmra	0.0373232
parallax_pmde_corr		correlation between parallax and pmde	0.035907157
pmra_pmde_corr		correlation between pmra and pmde	0.0013401698
chisq		chi squared of astrometric fit	336.16397
uwe		unit weight error of astrometric fit	0.9731088
phot_z_mean_mag	mag	mean Z band magnitude	16.75006
phot_z_std_mag	mag	standard deviation of Z band magnitude	0.021935267
phot_z_n_epochs		number of Z band epochs contributing to statistics	8
z_n_obs		approximate number of Z band observations	9
z_n_det		number of Z band detections	9
z_n_amb		number of Z band detections shared with another source	0
phot_y_mean_mag	mag	mean Y band magnitude	15.495929
phot_y_std_mag	mag	standard deviation of Y band magnitude	0.016722715
phot_y_n_epochs		number of Y band epochs contributing to statistics	10
y_n_obs		approximate number of Y band observations	11
y_n_det		number of Y band detections	11
y_n_amb		number of Y band detections shared with another source	0
phot_j_mean_mag	mag	mean J band magnitude	14.492317
phot_j_std_mag	mag	standard deviation of J band magnitude	0.011483114
phot_j_n_epochs		number of J band epochs contributing to statistics	5

j_n_obs		approximate number of J band observations	6
j_n_det		number of J band detections	6
j_n_amb		number of J band detections shared with another source	0
phot_h_mean_mag	mag	mean H band magnitude	13.750394
phot_h_std_mag	mag	standard deviation of H band magnitude	0.014054991
phot_h_n_epochs		number of H band epochs contributing to statistics	5
h_n_obs		approximate number of H band observations	6
h_n_det		number of H band detections	6
h_n_amb		number of H band detections shared with another source	0
phot_ks_mean_mag	mag	mean Ks band magnitude	13.21982
phot_ks_std_mag	mag	standard deviation of Ks band magnitude	0.019139782
phot_ks_n_epochs		number of Ks band epochs contributing to statistics	141
ks_n_obs		approximate number of Ks band observations	184
ks_n_det		number of Ks band detections	180
ks_n_amb		number of Ks band detections shared with another source	0
ks_first_epoch	d	epoch of first Ks band detection	55260.36376
ks_last_epoch	d	epoch of last Ks band detection	58717.0649
ks_skew		skewness of Ks band magnitudes	0.6108212
ks_p0	mag	0th percentile (i.e. min) of Ks band magnitudes	13.172082
ks_p1	mag	1st percentile of Ks band magnitudes	13.1780205
ks_p2	mag	2nd percentile of Ks band magnitudes	13.185369
ks_p4	mag	4th percentile of Ks band magnitudes	13.191636
ks_p5	mag	5th percentile of Ks band magnitudes	13.193609
ks_p8	mag	8th percentile of Ks band magnitudes	13.197648
ks_p16	mag	16th percentile of Ks band magnitudes	13.20169
ks_p25	mag	25th percentile of Ks band magnitudes	13.206783
ks_p32	mag	32nd percentile of Ks band magnitudes	13.210841
ks_p50	mag	50th percentile (i.e. median) of Ks band magnitudes	13.217017
ks_p68	mag	68th percentile of Ks band magnitudes	13.2265835
ks_p75	mag	75th percentile of Ks band magnitudes	13.231348
ks_p84	mag	84th percentile of Ks band magnitudes	13.238225
ks_p92	mag	92nd percentile of Ks band magnitudes	13.245653
ks_p95	mag	95th percentile of Ks band magnitudes	13.2479105
ks_p96	mag	96th percentile of Ks band magnitudes	13.249347

ks_p98	mag	98th percentile of Ks band magnitudes	13.267736
ks_p99	mag	99th percentile of Ks band magnitudes	13.27843
ks_p100	mag	100th percentile (i.e. max) of Ks band magnitudes	13.288555
ks_mad	mag	median absolute deviation from the median Ks band magnitude	0.012143135
ks_med_err	mag	median uncertainty of Ks band magnitudes	0.0201695
ks_Stetson_I		Stetson I index for Ks band magnitudes	0.2157366304
ks_Stetson_J		Stetson J index for Ks band magnitudes	0.1349608736
ks_Stetson_K		Stetson K index for Ks band magnitudes	0.8183742497
ks_Stetson_group_count		number of observation groups used for Stetson indices	61
ks_eta		von Neumann eta index	1.564529302
ks_eta_f		modified von Neumann eta index	1051447887

VVVX_VIRAC_V2_LC and VVVX_VIRAC_V2_REJECTED_LC table schema:

Column names, units and descriptions for the light curve tables. An example row is also given, that of the first time series element for the example source shown in the source table schema above. The *sourceid* field links to the source table, and the *catid* field links to the observation table (see below). This format is the same for both the main and reject tables.

Column Label	Units	Description	Example Row
sourceid		unique source identifier	15869033004249
catid		unique observation identifier	120741
mjdobs	d	epoch of observation	55260.36375826
filter		observation bandpass name	Ks
seeing	arcsec	observation seeing	0.624116289
ra	deg	right ascension	229.33949898506464
de	deg	declination	-58.85866266424065
era	mas	error on right ascension	7.892984765147925
edec	mas	error on declination	9.436603552353597
mag	mag	magnitude	13.245622
emag	mag	error on magnitude	0.021564407
phot_flag		photometric error flag	0
x	pixel	detector X position	1152.587
y	pixel	detector Y position	918.431
ex	pixel	error on detector X position	0.023
ey	pixel	error on detector Y position	0.02
cnf_ctr		CASU confidence value of centroid pixel	95
chi		dophot chi of detection	2.52

objtype		dophot object type	1
ext		VIRCAM detector number	13
ast_res_chisq		chi squared of astrometric residual	4.3247724
ambiguous_match		flag indicating shared detection	0

VVVX_VIRAC_V2_OBS table schema:

Column names, units and descriptions for the observation index table. An example row is also given, that of the observation corresponding to the time series element shown in the light curve table schema above. The *catid* field links to the light curve table.

Column Name	Units	Description	Example Row
catid		unique observation identifier	120741
filename		FITS filename of the image	v20100304_00780_st.fits.fz
tile		VVV tile name	d018
ob		OB name	d018v-1
filter		filter name	Ks
ra	deg	right ascension	228.858112
de	deg	declination	-59.48647
l	deg	galactic longitude	320.302109749199
b	deg	galactic latitude	-1.56127378157683
exptime	s	exposure time	4.0
mjdobs	d	MJD of observation	55260.36375826
airmass		airmass	1.222
skylevel		sky level (CASU)	4981.22
skynoise		sky noise (CASU)	45.515
elliptic		ellipticity (CASU)	0.10192925
seeing	arcsec	seeing	0.624116289

Acknowledgements

Please cite the VIRAC2 paper (Smith et al. 2025, MNRAS [insert ref]) and add the following acknowledgement to articles which use data from this release:
"based on data products from VVV Survey (programme ID 179.B-2002) and VVVX Survey (programme ID 198.B-2004) observations made with the VISTA telescope at the ESO Paranal Observatory"

According to the Data Access Policy for ESO data held in the ESO Science Archive Facility, all users are required to acknowledge the source of the data with appropriate citation in their publications.

Since processed data downloaded from the ESO Archive are assigned Digital Object Identifiers (DOIs), the following statement must be included in all publications making use of them:

- *Based on data obtained from the ESO Science Archive Facility with DOI:* https://doi.eso.org/10.18727/archive/67 (VVV) and https://doi.eso.org/10.18727/archive/68 (VVVX).

Publications making use of data which have been assigned an archive request number (of the form XXXXXX) must include the following statement in a footnote or in the acknowledgement:

- *Based on data obtained from the ESO Science Archive Facility under request number <request_number>.*